David S. Kuponiyi, Matthew B. Olajide,
Michael A. Eko, Charity S. Odeyemi,
Najeem O. Adelakun

Design Analysis of Microgrid Power System for Telecommunication Industries in Nigeria

DAVID S. KUPONIYI[1], MATTHEW B. OLAJIDE[2], MICHAEL A. EKO[3], CHARITY S. ODEYEMI[4], NAJEEM O. ADELAKUN[5]

[1,3]Department of Electrical/Electronic Engineering, Gateway (ICT) Polytechnic, Saapade, Ogun State NIGERIA

[2]Department of Electrical/Electronic Engineering, Olabisi Onabanjo University Ago-Iwoye, Ogun State, NIGERIA

[4]Department of Electrical/Electronic Engineering, Federal University of Technology Akure, Ondo State, NIGERIA

[5]Department of Works and Services, Federal College of Education Iwo, Osun State NIGERIA

Abstract: - A microgrid power system is an independent power system that provides off-grid power or grid backup. It consists of a conventional power system, a renewable power system, power storage, load management, and a control system. However, different microgrid configurations do exist, be it conventional energy sources or hybrid energy configurations, which have been discussed in this research to achieve an efficient and cost-competitive power system configuration. The microgrids could improve the quality of service for the telecommunications industries in Nigeria. The study takes into account the diverse network architecture of eight possible configured network models, and the topologies were simulated and tested for economic optimisation on HOMER energy software. The simulation results show that if any of the options were properly studied and harnessed, a permanent solution to power failure at our base station would be achieved. Similarly, the cost analysis presented reveals that the installation and operating expenses of any of the options were relatively cheap when compared to conventional procedures, lowering the tariff cost imposed on customers. Consequently, it will lead to the development of robust, off-grid power solutions for telecom infrastructure, enabling continuous connectivity in remote locations, decreasing downtime, and improving the country's digital communication network.

Key-Words: - microgrid, renewable energy, power system, modeling, network topology, simulation.

1 Introduction

With increased penetration in the country's rural regions, Nigeria's telecommunications sector has continued to expand enormously, requiring a stable energy supply capable of powering mobile base stations in an environmentally acceptable way. Rural electrification may be accomplished through three methods: extension of existing national grids, minigrids or microgrids, and freestanding power microgeneration systems [1]. Due to the growing usage of renewable energy sources (RES) and the country's inconsistent electricity supply, Nigeria's electrical infrastructure requires renovation [2–3]. However, the country's erratic power supply has impeded telecommunications carriers' ability to deliver high-quality service. This demands the need for alternative energy sources that can improve power quality, give rapid access to electricity, promote reliable, energy-efficient, and renewable energy, and provide a variety of eco-friendly benefits over existing utility systems [4]. Thus, renewable energy has gradually become a viable option for both developed and developing countries in terms of energy challenges, with solar energy performing as a major source of growth [5-8].

Globally, the networking industry has expanded at a rapid pace in recent years, resulting in a massive increase in the number of wireless devices. However, energy consumption is one of the most expensive

David S. Kuponiyi, Matthew B. Olajide,
Michael A. Eko, Charity S. Odeyemi,
Najeem O. Adelakun

elements for telecommunications providers [9], and the demand for energy will increase as more traffic load is expected in forthcoming 5G networks [10]. It is also worth noting that base stations (BSs) are frequently regarded as key energy consumption elements of cell sites [11]. During the last two decades, there has been an increase in demand for base transceiver stations (BTSs) due to the growth of mobile communication networks with smaller cells and BTSs closer to consumers [12].

A microgrid is an interconnected network of distributed energy sources and loads that function as a single controlled entity in relation to the grid [13]. Microgrids are grid components that may operate autonomously and comprise distributed energy suppliers, distributed sensing, and demand-side control. The concept of microgrids was introduced by the Consortium for Electric Reliability Technology Solutions (CERTS), and many research and test beds have been done in both industrialised and developing nations since then [14]. The idea integrates renewable and conventional power sources to ensure: enhanced renewable energy contributing to local and grid-wide power demands; efficient blending of renewable power sources; and power supplies. Microgrids are classified as DC, AC, or hybrid microgrids [15], which play a vital role in the maintenance of the mobile network, with a benchmark network uptime of 99.98% to ensure reliability and quality of service [16–17]. Congestion is a fundamental issue in telecom quality of service (QoS), where congestion simply signals a shortage of network resources [18–19]. After more than twenty years of GSM, the quality of service has not kept pace with the increasing development in the telecom market, with different consumer complaints about paying for undelivered messages, cost for dropped calls, and so on [20].

The total number of base stations owned by mobile telecommunications companies increased to 30,637 in December 2018 from 30,598 in December 2017, representing a 6.02% increase over the previous year across all states of the Federation. MTN had 14,715 base stations in December 2018, followed by AIRTEL (7,966), GLO (7,244), NTEL (562), EMTS (148), and SMILE (2 base stations) [21]. Several telecom businesses went with diesel generators with inverters and battery banks as backups to prevent unpredictable power from the national grid. As a result, carbon monoxide (Co) pollution developed. Energy efficiency in communication networks looks to be an absolute requirement in the battle against global warming [22].

To increase service quality without interruption, several attempts have been made to power telecommunications base stations using hybrid power systems, micropower systems, and other renewable sources. It is worth noting that integrating artificial intelligence (AI) algorithms into the microgrid power system framework can provide real-time load forecasting and adaptive energy management, optimising microgrid performance and providing uninterrupted power supply to telecom infrastructure [23]. [24] conducted energy audits on various telecommunication base stations (BTS) in Cameroon's Sahel area to assess and create an optimisation framework that reduces the operational costs of several BTS power system combinations, including utility grids with battery backup, utility grids with battery backup and diesel generators, and utility grids with battery backup and solar. The data revealed that the utility grid combination with a diesel generator and battery bank is more expensive, particularly when the 8-hour window is taken into account, costing up to $12.86 in comparison to $12.44 and $10.54 for configurations 1 and 3, respectively.

Despite the bold action of the operators, the power supply problem remains owing to high diesel costs, theft, and other socioeconomic concerns associated with the operation and maintenance of diesel generator sets, as well as national grid instability. The price of fuel jumped to N836.81 per litre in March 2023 from N539.32 in the same month in 2022, according to the National Bureau of Statistics [25–26]. As a result, this study used HOMER energy software for the research analysis. Hybrid Optimisation Model for Electric Renewable (HOMER) is a simulation model software for comparing and assessing micro-grid technologies for a wide range of applications [7], and it may simulate hundreds of systems depending on how the problem is framed. The Hybrid Optimisation Model for Electric Renewable (HOMER) is a simulation model software for evaluating and analysing micro-grid technologies for a wide range of applications, and it can simulate hundreds of systems depending on how the problem is phrased.

2 Design Principle

The microgrid system components are interconnected as indicated in Figures 1–8 to allow modelling and optimisation of the entire system. The systems also include energy storage in batteries to extend the length of energy autonomy, as well as a backup diesel generator connected to the system to provide electric energy for peak loads that cannot be handled by the renewable system.

This section discusses modelling and sizing, which are also dependent on the requirements of the load and the power supply system. Consequently, the proper size of microgrid system components is

David S. Kuponiyi, Matthew B. Olajide,
Michael A. Eko, Charity S. Odeyemi,
Najeem O. Adelakun

calculated such that the power system is neither excessive (expensive without boosting performance) nor undersized (unable to operate loads). This study also takes into account the diverse network architecture of eight possibilities that have been studied and tested for economic optimisation.

2.1 Network Topologies

The eight options considered are as follows: the first option uses only a diesel generator set to provide power without any other components; the second option uses a solar energy source, a diesel generator set, and a bi-directional inverter without a battery; and the remaining options are highlighted below.

Regarding the characteristics of the primary load, a suitable size of modelled components was simulated for each network design for optimised results discussed later in this study.

Figure 1 - Network with only diesel genset source Microgrid Network Diagram (option 1)
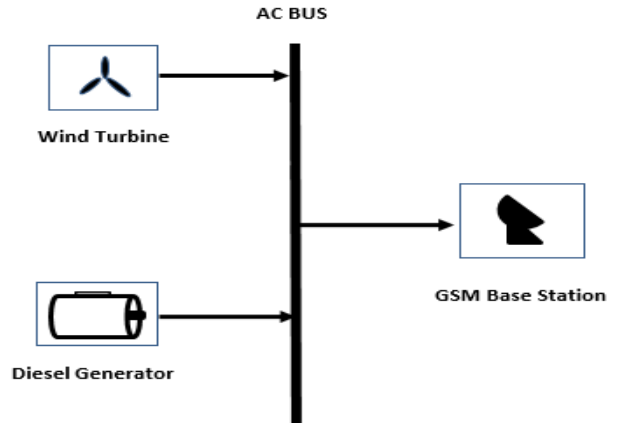
Figure 4 - Network without DC bus Microgrid Network Microgrid Network Diagram (option 4)
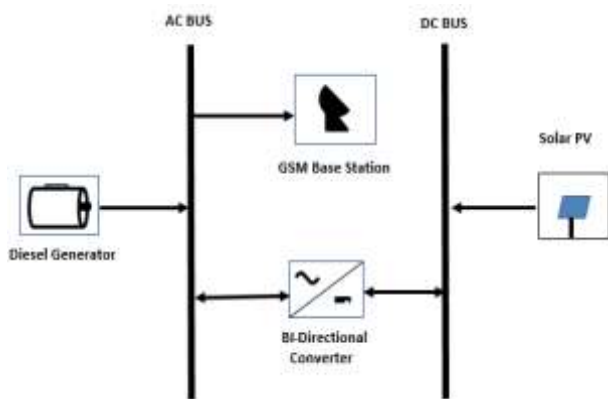
Figure 2 - Network without wind turbine and storage battery Microgrid Network Diagram (option 2)
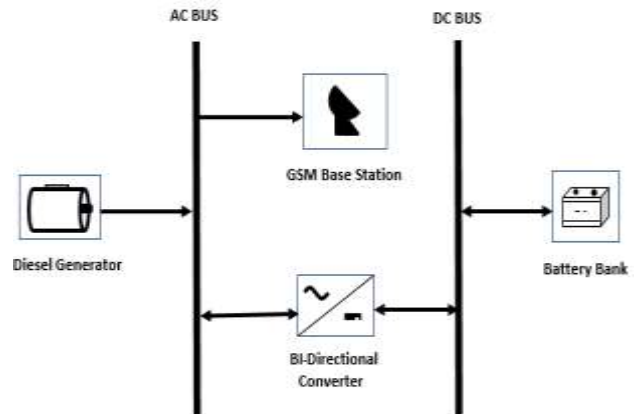
Figure 5 - Network without without renewable source Microgrid Network Diagram (option 5)
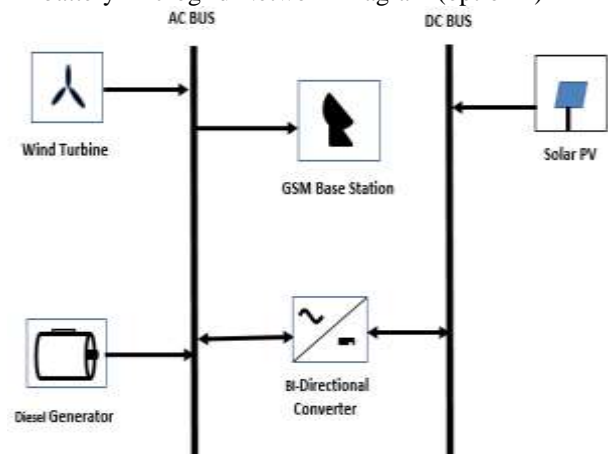
Figure 3 - Network without storage battery only Diagram (option 3)
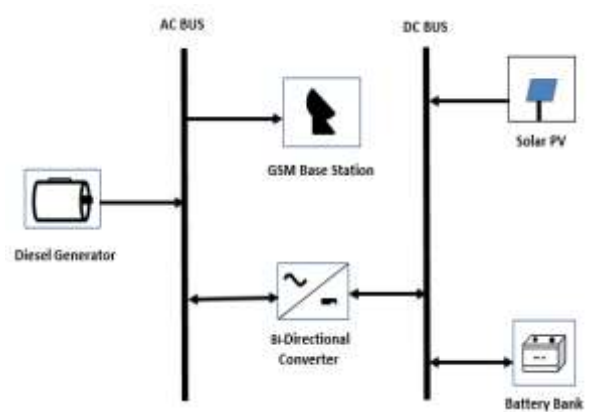
Figure 6 - Network without wind energy source only Microgrid Network Diagram (option 6)

David S. Kuponiyi, Matthew B. Olajide,
Michael A. Eko, Charity S. Odeyemi,
Najeem O. Adelakun
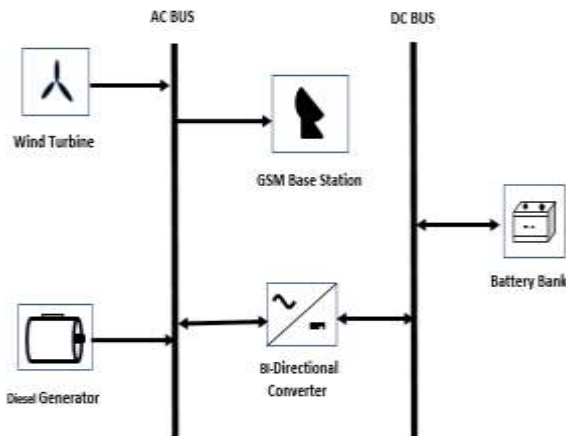
Figure 7 - Network without PV solar panel Microgrid Network Diagram (option 7)
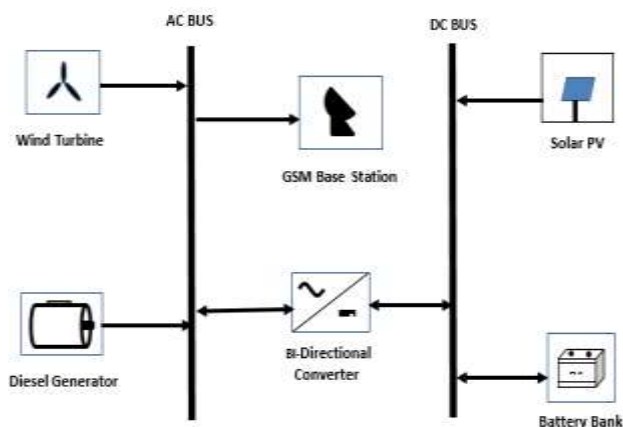
Figure 8 - Network considered Microgrid Network Diagram (option 8)

2.1.1 Components Modeling and Sizing Analysis

A. Primary Load and Profile

To avoid unmet demand, the electrical load known as the primary load must be satisfied immediately. The system may accept the addition of two or more separate primary loads via the Add/Remove window, but only one is considered for this project, with all DC loads drawing power from the AC bus via individual power rectifier units. Every hour of the year, power from the system's power-producing modules is sent out to serve the complete primary load.

The daily load profile utilised is based on an informed estimate, with the maximum load of the BTS shown in Table 1. Typically, BTS load profiles peak in the morning near a business metropolis and in the evening and on weekends near a residential area. Though it is critical to have a solid estimate of the load demand since it will impact the size of the microgrid components (generators, battery bank, and converter).

B. BTS Energy Demand

The initial step was to determine the energy requirement of the BTS under consideration. This was accomplished by evaluating the influence of several operational systems that comprise a BTS, with a BTS serving as a model. A BTS is a tower or mast equipped with telecommunications technology to broadcast mobile signals (voice and data), such as an antenna, radio reception, and transmitters at the top of the mast [25], and is often referred to as a primary energy requirement part of mobile telecommunication networks that facilitates wireless communications between user equipment and a network [27]. At the foot of each tower is a shelter with extra gearbox equipment, air conditioning, battery banks, and a diesel generator for BTS in off-grid situations [25]. The BTS site load profile is influenced by radio equipment, antennas, power conversion equipment, and transmission equipment, among other things. As a result, it is necessary to develop an accurate power profile before selecting and sizing energy components. The categories below indicate how much energy each component consumes at a typical Radio Base Station (RBS) location [25].

1. Radio equipment:
   - Radio Unit (RF Power Amplification and Radio Frequency (RF) Conversion) = 4210W
   - Base Band (Processing and Control Signal) = 2190 W

2. Power equipment:
   - Power Supply with Rectifier = 1200W

3. Antenna equipment:
   - RF feeder = 120W
   - Remote Monitoring and Safety Lamp = 100W

4. Transmission equipment:
   - Transmitter (signal) = 120W

5. Auxiliary equipment
   - Security and Lighting = 200 W
   - Temperature control equipment (air conditioner) = 1500W (2H.P.)

David S. Kuponiyi, Matthew B. Olajide,
Michael A. Eko, Charity S. Odeyemi,
Najeem O. Adelakun

Based on the above, a typical hourly-daily load profile for the base station was evaluated using the maximum load to guarantee adequate size of the energy sources. The primary load profile input for simulation is shown in Table 1.

Table 1: Typical Load Demand For A Base Transceiver Station

BTS HOURLY - DAILY LOAD DEMAND									
Hourly Time	Radio Unit (W/h)	Base Band Unit (W/h)	Power Supply with Rectifier (W/h)	RF Feeder Unit (W/h)	Remote Monitoring and Safety Lamp	Signal Transmitter (W/h)	Security and Lighting (W/h)	Temperature Control Equipment (W/h)	Total (W/h)
00-01	4210	2190	1200	120	100	120	200	900	9040
01-02	4210	2190	1200	120	100	120	200	900	9040
02-03	4210	2190	1200	120	100	120	200	900	9040
03-04	4210	2190	1200	120	100	120	200	900	9040
04-05	4210	2190	1200	120	100	120	200	900	9040
05-06	4210	2190	1200	120	100	120	200	900	9040
06-07	4210	2190	1200	120	100	120	200	900	9040
07-08	4210	2190	1200	120	100	120	OFF	900	8840
08-09	4210	2190	1200	120	100	120	OFF	900	8840
09-10	4210	2190	1200	120	100	120	OFF	1125	9065
10-11	4210	2190	1200	120	100	120	OFF	1125	9065
11-12	4210	2190	1200	120	100	120	OFF	1125	9065
12-13	4210	2190	1200	120	100	120	OFF	1500	9440
13-14	4210	2190	1200	120	100	120	OFF	1500	9440
14-15	4210	2190	1200	120	100	120	OFF	1500	9440
15-16	4210	2190	1200	120	100	120	OFF	1500	9440
16-17	4210	2190	1200	120	100	120	OFF	1500	9440
17-18	4210	2190	1200	120	100	120	OFF	1500	9440
18-19	4210	2190	1200	120	100	120	200	1500	9640
19-20	4210	2190	1200	120	100	120	200	1125	9265
20-21	4210	2190	1200	120	100	120	200	1125	9265
21-22	4210	2190	1200	120	100	120	200	1125	9265
22-23	4210	2190	1200	120	100	120	200	1125	9265
23-00	4210	2190	1200	120	100	120	200	1125	9265
Total	**101040**	**52560**	**28800**	**2880**	**2400**	**2880**	**2600**	**27600**	**20760**

C. Energy Resources

The term "resource" refers to everything that comes from outside the power system and is used by it to create electric or thermal power. The four basic renewable energy sources are solar, wind, hydro, and biomass, and any fuel required by the system's

David S. Kuponiyi, Matthew B. Olajide,
Michael A. Eko, Charity S. Odeyemi,
Najeem O. Adelakun

components is included. The placement of renewable resources has a large impact. Large-scale atmospheric circulation patterns and geographic effects influence the wind resource; local rainfall patterns and terrain influence the hydro resource; and regional biological productivity influences both the hydro and solar resources. Furthermore, a renewable resource may demonstrate significant hour-to-hour and seasonal variations at any one place. Because the resource determines renewable energy output, the type of renewable resources available has an impact on the economics and behaviour of renewable energy systems. As a result, accurate modelling of renewable resources has become an essential component of system modelling. This section explains how HOMER models fuel and renewable resources.

D. Wind Turbine Modelling and Sizing

Modelling wind turbines with HOMER requires the input of the type of turbine if it is not already in the library. Also considered for modelling is the input cost of turbine sizes, which is very important for simulation. HOMER provides different drop-down boxes and tables for these options.

E. Wind Turbine Sizing

i. Wind Turbine type

All of the many varieties of wind turbines that are kept in the component library are available in this drop-down box. From this list, a suitable wind turbine model is picked. Following your choice from this drop-down box, a brief description of the chosen wind turbine's characteristics is shown in the area below, and you may view more information by clicking the Details button.

Additionally, by selecting the new button, a brand-new sort of wind turbine may be developed. The new turbine type will be included in HOMER's component library. Alternatively, by selecting the Delete button, any turbine type can be eliminated from the component collection.

ii. Wind Turbine Properties

The main characteristics of the chosen wind turbine are displayed in this section. The power curve, which describes the output of the turbine's power over a range of wind speeds, is its most important characteristic. Using a standard wind turbine power curve, it was determined that the chosen wind turbine was suitable.

F. Modelling and Sizing of PV Panels

The total peak power of the PV generator needed to supply a specific load depends on the load, solar radiation, ambient temperature, power temperature coefficient, efficiencies of the solar charger regulator and inverter, as well as the safety factor taken into account to account for losses and temperature effect. This total peak power is obtained as follows

$$P_{PV} = Y_{PV}f_{PV}\left[\frac{\bar{G}_T}{\bar{G}_{T,STC}}\right][1 + \alpha_P(T_C STC)] \tag{1}$$

Where:

Y_{PV} is the PV array's rated capacity, i.e., its power production under typical test conditions. (kW)

f_{PV} is the PV derating factor (%)

$\bar{G}_T$ Is solar radiation hitting the PV array at the present time step? (kW/m^2)

$\bar{G}_{T,STC}$ Is the radiation incident under typical test conditions? (1 kW/m^2)

α_P is the coefficient of power for temperature (% / °C)

T_c is the temperature of PV cell at this moment in time (°C)

$T_{c,STC}$ is the PV cell temperature understandard conditions (25 °C)

As the influence of temperature on the PV array is not selected in the PV Inputs box for this project, HOMER assumes that the temperature coefficient of power is zero, simplifying the preceding equation to:

$$P_{PV} = Y_{PV}f_{PV}\left[\frac{\bar{G}_T}{\bar{G}_{T,STC}}\right] \tag{2}$$

G. Modeling and Sizing of Battery Bank

As the wind speed changes throughout the day, so does the wind turbine's output power. Additionally, fluctuations in solar light and temperature affect the maximum power

David S. Kuponiyi, Matthew B. Olajide,
Michael A. Eko, Charity S. Odeyemi,
Najeem O. Adelakun

output of the PV generator. Therefore, it's possible that the wind turbine and the PV generator won't always be able to handle the load. During these periods, a battery placed between the microgrid system's DC bus and the load will serve as a power supply and compensate.

When the output power from the wind turbine and PV generator exceeds the amount of power needed for the load, the excess energy is stored in the battery to provide power for the load when the wind turbine and PV generator are unable to do so.

The battery capacity considered in this research is determined by (3) and (4).

$$BC = \frac{2 \times f \times W}{Vbatt} \qquad (3)$$

Where

BC is the capacity of a battery
F is the the reserve factor
W is the Daily Energy demand
Vbatt is the DC Bus voltage for the system

The battery's Ampere-hour (Ah) rating is calculated as

$$Ah = \frac{Daily\ Energy\ Consumption\ (kWh)}{Battery\ rating\ in\ (Amp-hr)\ at\ a\ specified\ voltage} \qquad (4)$$

H. Battery Bank

A grouping of one or more different batteries makes up the battery bank. A single battery is modelled by HOMER as a system that can store a specific amount of direct current electricity at a fixed round-trip energy efficiency, with restrictions on how quickly it can be charged or discharged, how deeply it can be discharged without suffering damage, and how much energy can cycle through it before it needs to be replaced. HOMER makes the assumption that a battery's characteristics will not change over the course of its lifetime due to environmental conditions like temperature.

The battery's nominal voltage, capacity curve, lifetime curve, minimum state of charge, and round-trip efficiency are its primary physical characteristics in HOMER. The capacity curve compares the battery's ampere-hours of discharge capacity to its amperes of discharge current. The amount of ampere-hours that can be discharged out of a fully charged battery at a steady current is what manufacturers use to calculate each point on this curve. Typically, capacity declines as discharge current rises. The battery's lifetime curve plots the number of discharge-charge cycles it can sustain against the depth of the cycle. As cycle depth increases, the number of cycles to failure often decreases. The minimum state of charge is the state of charge below which the battery must not be discharged in order to prevent long-term harm. In the system simulation, HOMER prevents the battery from being depleted more deeply than this threshold. The amount of

energy entering the battery that can be pulled out again is indicated by the round-trip efficiency.
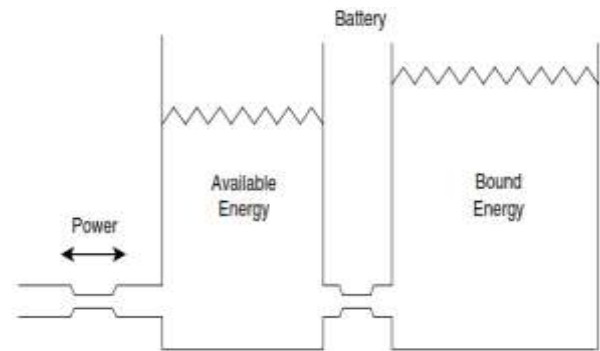
Figure 9 - Kinetic Battery Model [28]

The kinetic battery model [28], which treats the battery as a two-tank system as depicted in Figure 9, is used by HOMER to determine the battery's maximum permitted rate of charge or discharge. The kinetic battery concept states that while some of the battery's energy storage capacity is instantaneously accessible for charging or discharging, the other portion is chemically bonded. The difference in height between the two tanks affects how quickly available energy is converted into bound energy. The battery can be described by three variables. The total size of the available and bound tanks is the battery's maximum capacity. The ratio of the size of the available tank to the total size of the two tanks is referred to as the capacity ratio. The pipe size between the tanks and the rate constant are comparable.

The shape of the usual battery capacity curve, such as the one in Figure 10, is explained by the kinetic battery model. High discharge rates cause the available tank to quickly empty, and very little of the bound energy can be released before the tank is empty. At this point, the battery is no longer able to sustain the high discharge rate and seems to be totally depleted. The apparent capacity rises when the discharge rate slows because more bound energy can be converted to usable energy before the available tank is completely depleted. The three components of the kinetic battery model are calculated by HOMER using a curve fit on the battery's discharge curve. In accordance with this curve fit, the line in Figure 10 is drawn.

It contains two effects to model the battery as a two-tank system rather than a single-tank system. It first implies that the battery cannot be fully charged or drained simultaneously; a full charge necessitates an infinite amount of time at a charge current that asymptotically approaches zero. Second, it implies that the battery's capacity to charge and discharge is influenced not only by its current level of charge but also by its most recent history of charge and discharge. Since it will have a larger level in its available tank, a battery that has been rapidly charged to 80 percent state of charge can discharge at a quicker pace than the same battery that has been similarly rapidly discharged to 80 percent. Each hour, HOMER monitors the levels in the two tanks and models both of these impacts.

David S. Kuponiyi, Matthew B. Olajide,
Michael A. Eko, Charity S. Odeyemi,
Najeem O. Adelakun
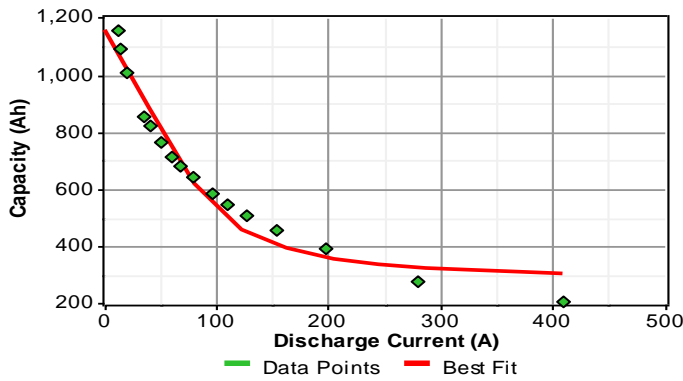
Figure 10 - Cappacity Curve Of The Battery

Figure 11 - Lifetime Curve For The Modelled Battery

A deep-cycle lead-acid battery lifetime curve is depicted in Figure 10. With increasing discharge depth, the number of cycles before failure (shown on the graph as the lighter-colored spots) rapidly decreases. Finding the product of the number of cycles, the depth of discharge, the nominal voltage of the battery, and the aforementioned maximum capacity of the battery allows one to determine the lifetime throughput (the amount of energy that passed through the battery before failure) for each point on this curve. Figure 11's lifetime throughput curve, shown as a series of black dots, frequently depends on cycle depth far less. HOMER's simplifying premise is that the depth of discharge has no impact on lifetime throughput. The average of the points from the lifespan curve above the minimal state of charge is the value that HOMER recommends for this lifetime throughput, although the user can change this number to be more or less conservative.

Assuming that lifetime throughput is independent of cycle depth, HOMER may predict the battery bank's remaining life by observing the quantity of energy passing through it, without taking the length of the numerous charge-discharge cycles into account. HOMER determines the battery bank's lifespan in years as

$$R_{batt} \;=\; \min\left(\frac{N_{batt}\,Q_{lifetime}}{Q_{thrpt}},\, R_{batt,f}\right) \qquad (5)$$

where

N_{batt} is the number of batteries in the battery bank,

$Q_{lifetime}$ the lifetime throughput of a single battery,

Q_{thrpt} the annual throughput (the total ammount of energy that cycles through the battery bank in one year) and

$R_{batt,f}$ the float life of the battery (the maximum life regardless of throughput).

The capital cost, replacement cost, and Operations and maintenance cost of the battery bank are all stated in US dollars (HOMER standard) each year. As a dispatchable power source, the battery bank's fixed and marginal energy costs are calculated for comparison with those of other dispatchable sources. The fixed cost of energy for the battery bank is zero because, unlike the generator, it doesn't cost anything to run it so that it is ready to produce energy. HOMER calculates the marginal cost of energy as the product of the battery wear cost (the price per kilowatthour for cycling energy through the battery bank) and the battery energy cost (the average cost of the energy stored in the battery bank). The battery wear cost is determined by HOMER as follows:

$$C_{bw} \;=\; \frac{C_{rep.batt}}{N_{batt}\,Q_{lifetime}\,\sqrt{\eta_{rt}}} \qquad (6)$$

where

$C_{rep.batt}$ is the replacement cost of the battery bank

N_{batt} is the number of batteries in the battery bank,

$Q_{lifetime}$ is the life time throughput of a single battery (kWh), and

η_{rt} is the round-trip efficiency.

By dividing the overall annual cost of charging the battery bank by the total annual quantity of energy put into the battery bank, HOMER determines the battery energy cost for each hour of the simulation. Due to the fact that the battery bank is only ever charged by excess electricity while using the load following dispatch technique, there is never any cost involved in doing so. The cost of charging the battery bank is not zero, however, because the cycle-charging approach calls for a generator to create extra energy (and hence use more fuel) specifically for the purpose of charging the battery bank.

David S. Kuponiyi, Matthew B. Olajide,
Michael A. Eko, Charity S. Odeyemi,
Najeem O. Adelakun
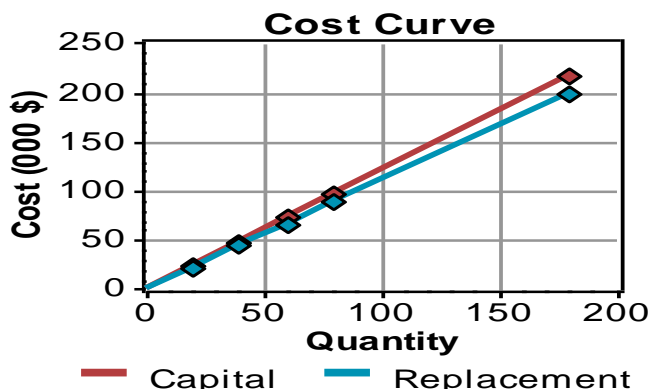
Figure 12 - Battery Sizing Cost Curve

I. Diesel Generator

Fuel is consumed by a diesel generator to generate power, along with potential heat output. The generator module in HOMER is adaptable enough to represent a wide range of generators, including those powered by internal combustion engines, microturbines, fuel cells, Stirling engines, thermophotovoltaic generators, and thermoelectric generators. As many as three generators, each of which may be ac or dc and use a different fuel, could be used in a power system that HOMER can simulate.

The generator's main physical characteristics include its maximum and minimum electrical power output, estimated lifetime in operating hours, the kind of fuel it uses, and its fuel curve, which connects the amount of fuel used to the amount of electrical power generated. The fuel consumption of the generator is calculated using the following equation by HOMER under the assumption that the fuel curve is a straight line with a y-intercept:

$$F = F_o Y_{gen} + F_1 P_{gen} \qquad (7)$$

Where
F_0 is the fuel curve intercept coefficient,
F_1 is the fuel curve slope,
Y_{gen} the rated capacity of the generator (kW), and
P_{gen} the electrical output of the generator (kW).

The measuring units for the fuel determine the units of F. The units of gasoline are L/h if the fuel is measured in liters. The units of F are m^3/h or kg/h depending on whether the fuel is expressed in m^3 or kilogram. Similarly, the units of F0 and F1 are determined by the fuel's measurement units. The units of F_0 and F_1 for fuels with liter denominators are L/h.kW. The user also specifies the heat recovery ratio for a generator that produces both heat and electricity. HOMER makes the assumption that the generator transforms 100% of the fuel energy into either waste heat or electricity. The amount of waste heat that can be recovered to meet the thermal load is known as the heat

recovery ratio. The modeler can also specify the generator emissions coefficients, which indicate the generator's emissions of six distinct pollutants in terms of grams of pollutant emitted per unit of fuel consumed.

The generator's functioning can be scheduled to turn on or off at predetermined times. When the generator isn't being pushed on or off, HOMER decides whether it should run based on the system's requirements and the relative costs of the alternative power sources. When the generator is required to run, HOMER chooses the power output level it will use, which might be anything between its minimum and maximum power output.

The initial capital cost in dollars, replacement cost in dollars, and annual Operations and maintenance cost in dollars per operating hour for the generator are all listed. Oil changes and other maintenance costs are included in the generator Operation and maintenance (o&m, but fuel prices are not included because fuel costs are determined separately by HOMER. The fixed and marginal cost of energy for the generator is determined, as it is for all dispatchable power sources, and used by HOMER to model the system operation. The hourly cost of simply running the generator without generating any electricity is the fixed cost of energy. The increased cost per kilowatthour for using that generator to produce power is known as the marginal cost of energy.

The fixed cost of energy for the generator is determined by HOMER using the following equation:

$$C_{gen.fixed} = C_{om.gen} + \frac{C_{rep.gen}}{R_{gen}} + F_o Y_{gen} C_{fuel.eff} \quad (8)$$

Where
$C_{om.gen}$ is the cost of running and managing in dollars per hour,
$C_{rep.gen}$ the replacement price in money,
R_{gen} is the generator life expectancy in hours,
F_0, the fuel curve intercept coefficient in terms of the fuel's quality per hour per kilowatt, and Ygen, the generator's capacity (kW), and
$C_{fuel.eff}$ the fuel's actual cost, expressed as a dollar amount per fuel quantity.

The effective price of fuel include the cost penalties if any associated with the emissions of pollutant from the generator.

The following equation is used by HOMER to determine the generator's marginal cost of energy:

$$C_{gen.mar} = F_1 C_{fuel.eff} \qquad (9)$$

where
F_1 is the fuel curve slope in quantity of fuel per hour per kilowatthour and $C_{fuel.eff}$ is the effective price of fuel (including the cost of any

David S. Kuponiyi, Matthew B. Olajide,
Michael A. Eko, Charity S. Odeyemi,
Najeem O. Adelakun

penalties on emissions) in dollars per quantity of fuel.

3 Simulation and Results

A. Simulation Input For BTS Energy Demand

Table 2: Simulation Input For BTS Energy Demand

AC Load: BTS PRY. LOAD	
Data source:	Synthetic
Daily noise:	19.70%
Hourly noise:	15.80%
Scaled annual average:	212 kWh/d
Scaled peak load:	17.0 kW
Load factor:	0.52
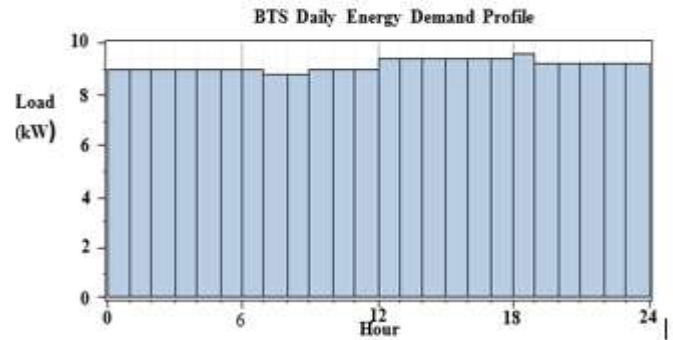
Figure13 - Typical Daily Energy Demand Profile of Base Station
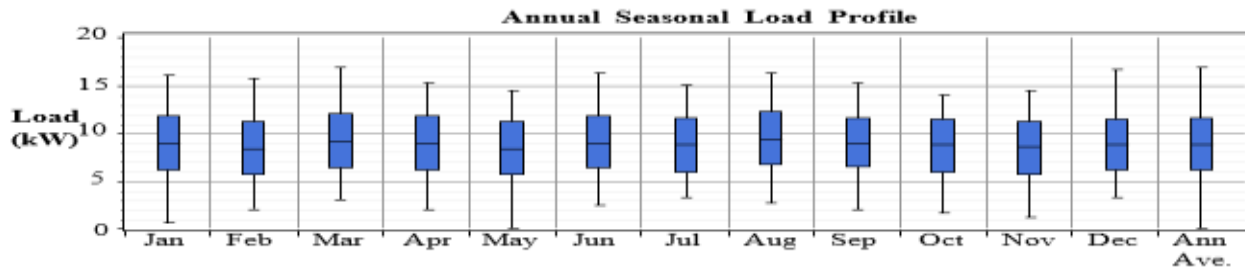
Figure14 - Typical Annual Load Profile of A BTS

A. Simulation Input for Solar PV

Table 3: Simulation Input for Solar PV

Size (kW)	Capital (₦)	Replacement (₦)	O&M (₦/yr)
1	412,500	330,000	0

Sizes considered:	10, 20, 30, 40, 60, 80 kW
Lifetime:	25 yr
Derating factor:	80%
Tracking system:	No Tracking
Slope:	6.57 deg
Azimuth:	0 deg
Ground reflectance:	20%

Solar Resource

Latitude:	6 degrees 42 minutes North
Longitude:	3 degrees 15 minutes East
Time zone:	GMT +1:00

David S. Kuponiyi, Matthew B. Olajide,
Michael A. Eko, Charity S. Odeyemi,
Najeem O. Adelakun

Synthesized Solar Radition Data

Month	Clearness Index	Average Radiation
		(kWh/m^2/day)
Jan	0.531	4.949
Feb	0.525	5.184
Mar	0.512	5.303
Apr	0.491	5.131
May	0.468	4.773
Jun	0.436	4.345
Jul	0.384	3.851
Aug	0.384	3.942
Sep	0.408	4.215
Oct	0.487	4.855
Nov	0.577	5.426
Dec	0.54	4.909
Scaled annual average:	4.74 kWh/m²/d	
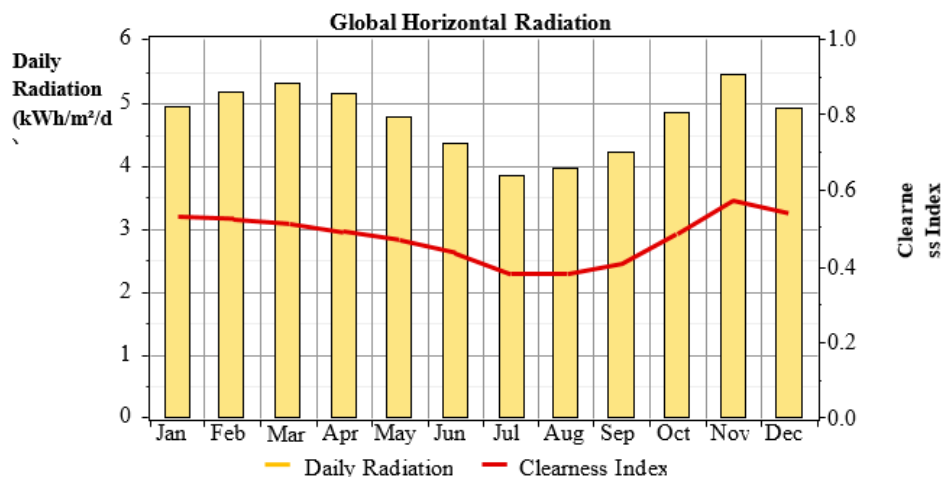
Figure 15 - Typical Global Horizontal Radiation for Sun

B. **Simulation Input for AC Wind Turbine: PGE 20/25**

Table 4: Simulation Input for AC Wind Turbine: 20/25

Quantity	Capital (₦)	Replacement (₦)	O&M (₦/yr)
1	7,260,000	6,660,000	74,250
Quantities to consider:	0, 1, 2, 3, 4		
Lifetime:	25 yr		
Hub height:	30 m		

Wind Resource

David S. Kuponiyi, Matthew B. Olajide,
Michael A. Eko, Charity S. Odeyemi,
Najeem O. Adelakun

Table 5: Synthesized Wind Speed Data

Month	Wind Speed
	(m/s)
Jan	4.15
Feb	4.3
Mar	4.01
Apr	3.49
May	3
Jun	3.12
Jul	3.7
Aug	3.85
Sep	3.5
Oct	2.83
Nov	3.05
Dec	3.65
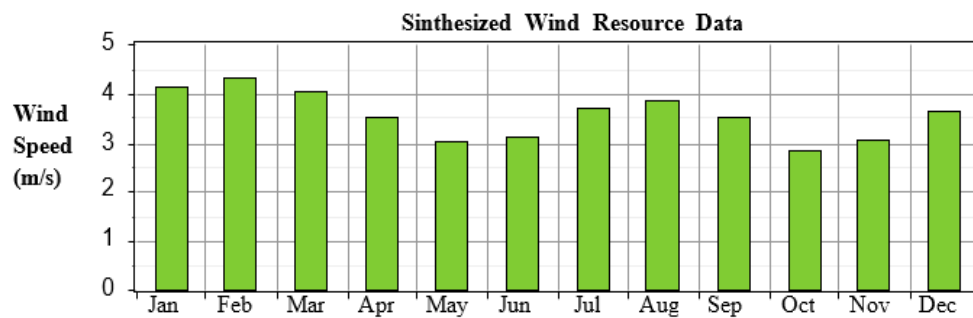
Figure 16 - Synthesized Wind Resource Data

Table 6: Other Simulation Input for AC Wind Turbine: 20/25

Weibull k:	2.01
Autocorrelation factor:	0.849
Diurnal pattern strength:	0.249
Hour of peak wind speed:	15
Scaled annual average:	3.55 m/s
Anemometer height:	50 m
Altitude:	30 m
Wind shear profile:	Logarithmic
Surface roughness length:	0.01 m

David S. Kuponiyi, Matthew B. Olajide,
Michael A. Eko, Charity S. Odeyemi,
Najeem O. Adelakun
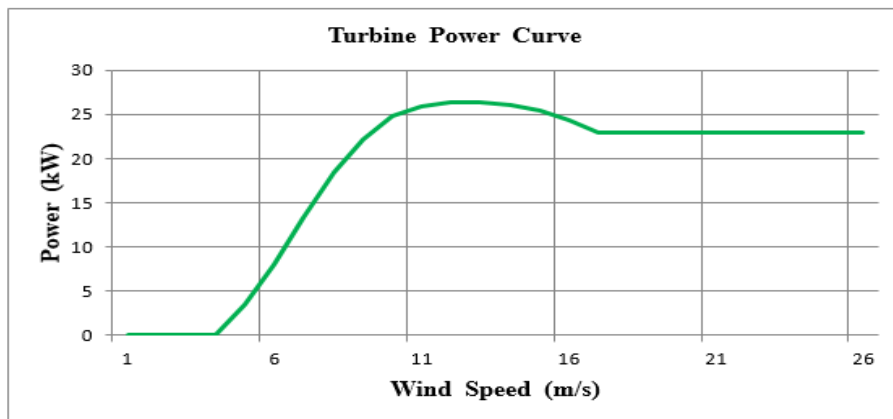
Figure 17 - Power Curve for Wind Turbine: 20/25

Wind Turbine Specification
Curve made at 25m hub height
Available towers: 24 / 30 / 36m
Rotor : 20m diameter, 305 m^2 swept, 32 rpm
Cold cut-in wind speed: 3.5 m/s
Low wind speed cut-out: 1.7 m/s
Rated power wind speed: 25 kW @ 9 m/s
High wind speed cut-out: 25 m/s

A.   Simulation Input for AC Generator: Generator 1

Table 7: Simulation Input for AC Generator

Size (kW)	Capital (₦)	Replacement (₦)	O&M (₦/hr)
22	3,234,000	2,640,000	825,000
44	4,867,500	4,125,000	1,155,000

Table 8: AC Generator Parameters/Specifications

Sizes to consider:	0, 22, 44 kW
Lifetime:	15,000 hrs
Min. load ratio:	30%
Heat recovery ratio:	0%
Fuel used:	Diesel
Fuel curve intercept:	0.08 L/hr/kW
Fuel curve slope:	0.25 L/hr/kW

David S. Kuponiyi, Matthew B. Olajide,
Michael A. Eko, Charity S. Odeyemi,
Najeem O. Adelakun
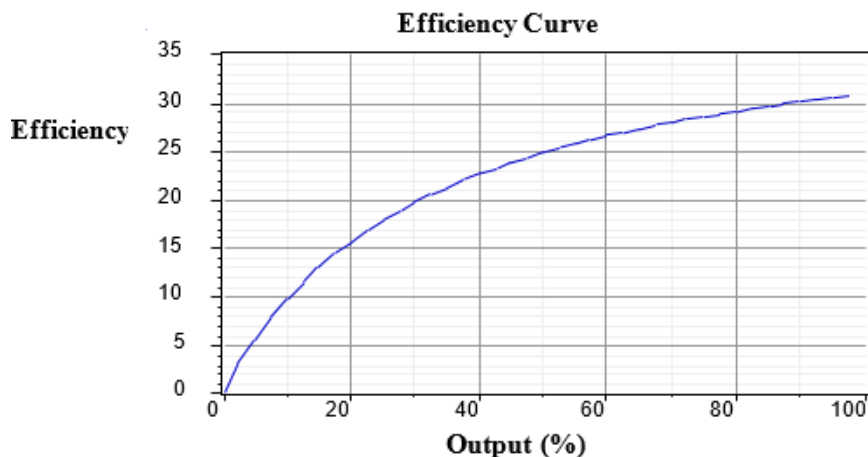
Figure 18 - Efficiency Curve for AC Generator 1

Table 9: Simulation Input for AC Generator Fuel: Diesel

Price:	(₦),99, 115.5, 132, 148.5, 165/L
Lower heating value:	43.2 MJ/kg
Density:	820 kg/m3
Carbon content:	88.00%
Sulfur content:	0.33%

C. Simulation Input for Battery: Surrette 6CS25P

Table 10: Simulation Input for Battery: Surrette 6CS25P

Quantity	Capital (₦)	Replacement (₦)	O&M (₦/yr)
1	198,000	181,500	8,250
Quantities considered:	0, 20, 40, 60, 80, 100		
Voltage:	6 V		
Nominal capacity:	1,156 Ah		
Lifetime throughput:	9,645 kWh		

D. Simulation Input for Converter: Bi-Directional

Table 11: Simulation Input for Bi-Directional Converter

Size (kW)	Capital (₦)	Replacement (₦)	O&M (₦/yr)
10	6,600,000	6,600,000	49,500
Sizes considered:		0, 5, 10, 20, 30, 40 kW	
Lifetime:		25 yr	
Inverter efficiency:		90%	
Inverter can parallel with AC generator:		Yes	
Rectifier relative capacity:		100%	
Rectifier efficiency:		85%	

David S. Kuponiyi, Matthew B. Olajide,
Michael A. Eko, Charity S. Odeyemi,
Najeem O. Adelakun

E. Simulation Optimised Result

Table 12: Optimization Result of Simulation.

TOPOLOGY	PV	W.T.	D.G.	BAT.	B.CON	T.C.C.	Total NPC	Operating Cost	COE	Ren. Fraction	Diesel	DGset Hours
	kW	Nr	kW	Nr	kW	₦	₦	₦/yr	₦/kWh		L/yr	hr/yr
OPTION 8	40	2	22	80	20	64,284,000	92,755,080	2,227,170	93.72	0.93	3,077	509
OPTION 7	0	2	22	40	10	33,264,000	102,585,945	5,422,890	103.785	0.55	17,748	2,941
OPTION 6	80	0	22	80	20	66,264,000	105,485,325	3,068,175	106.59	0.86	6,653	1,157
OPTION 5	0	0	22	40	10	18,744,000	134,917,530	9,087,870	136.455	0	32,634	5,268
OPTION 4	0	3	22	0	0	26,004,000	149,226,495	9,639,300	150.81	0.62	26,227	6,902
OPTION 3	30	3	22	0	10	44,979,000	149,559,135	8,181,030	151.14	0.74	21,757	5,843
OPTION 2	60	0	22	0	20	42,174,000	155,230,350	8,844,000	156.915	0.61	24,677	6,387
OPTION 1	0	0	22	0	0	4,224,000	159,794,745	12,169,740	161.535	0	35,168	8,759

The following table provides the optimisation outcome of all options assessed for this study, and the graphical summary analysis follows.

Graphical Summary Analysis of the Optimization

Figure 19 - Option 8 Cash Flow Analysis
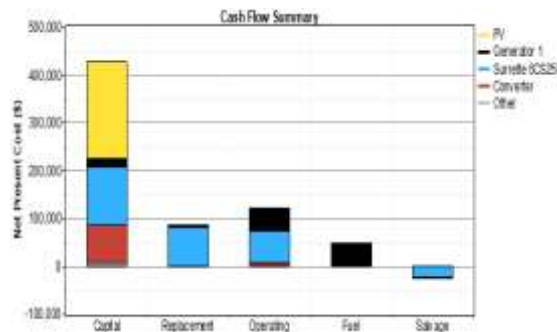
Figure 20 - Option 7 Cash Flow Analysis

David S. Kuponiyi, Matthew B. Olajide,
Michael A. Eko, Charity S. Odeyemi,
Najeem O. Adelakun
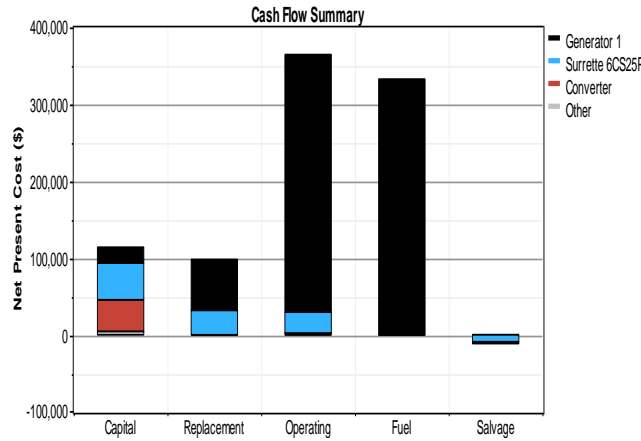
Figure 21 - Option 5 Cash Flow Analysis

Hourly - Daily Map (January)
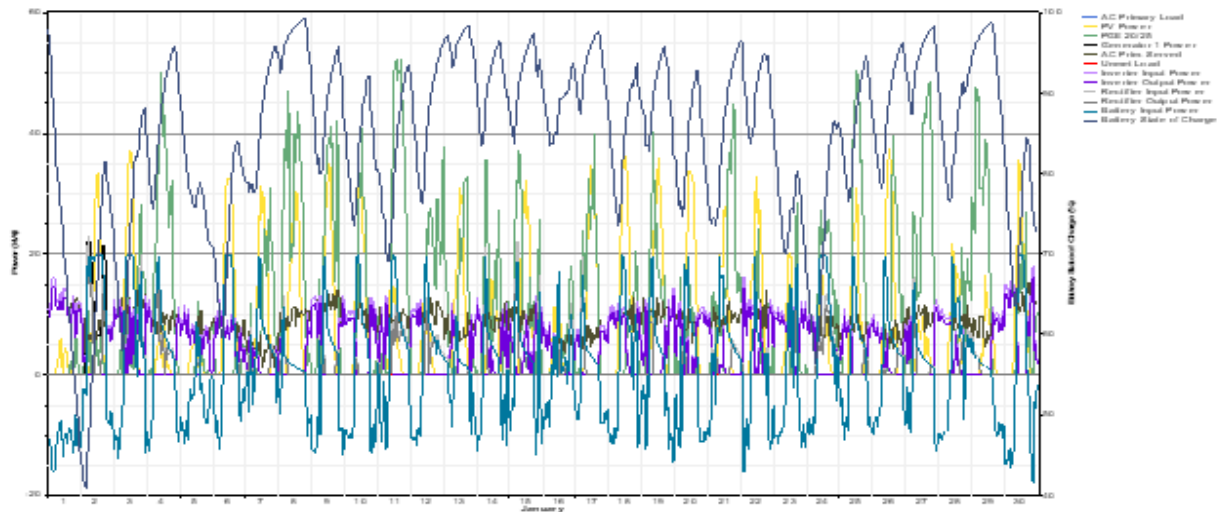
Figure 22 - Graphical Analysis For Hourly – Daily Map (January)

H. OTHER RESULTS
A. AC Wind Turbine: PGE 20/25

Table 13: Wind Turbine PGE 20/25 Output Analysis Result

Variable	Value	Units
Total rated capacity	50	kW
Mean output	6.97	kW
Capacity factor	13.9	%
Total production	61,015	kWh/yr
Variable	**Value**	**Units**
Minimum output	0	kW
Maximum output	52.4	kW
Wind penetration	78.9	%
Hours of operation	4,629	hr/yr
Levelized cost	0.128	$/kWh

David S. Kuponiyi, Matthew B. Olajide,
Michael A. Eko, Charity S. Odeyemi,
Najeem O. Adelakun
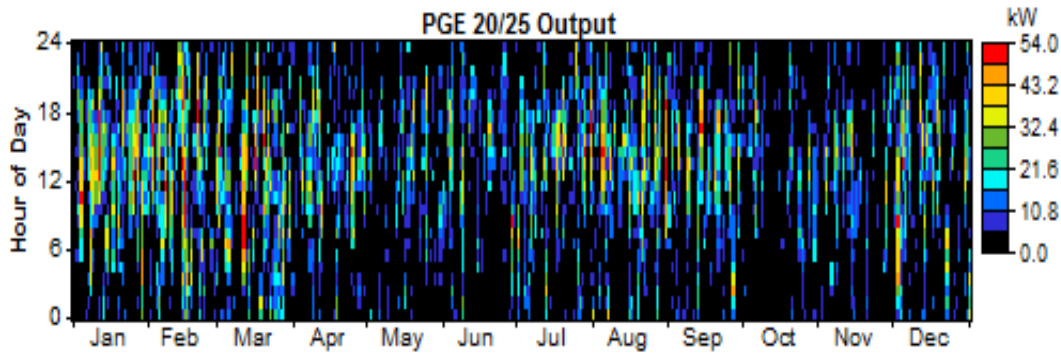
Figure 23 - Graphical Analysis For PGE 20/25 Output

B. Deisel Generator

Table 14: Diesel Generator 1 Output Analysis Result

Quantity	Value	Units
Hours of operation	526	hr/yr
Number of starts	31	starts/yr
Operational life	28.5	yr
Capacity factor	4.49	%
Fixed generation cost	7.47	$/hr
Marginal generation cost	0.2	$/kWhyr
Quantity	Value	Units
Electrical production	8,662	kWh/yr
Mean electrical output	16.5	kW
Min. electrical output	6.6	kW
Max. electrical output	22	kW
Quantity	Value	Units
Fuel consumption	3,091	L/yr
Specific fuel consumption	0.357	L/kWh
Fuel energy input	30,419	kWh/yr
Mean electrical efficiency	28.5	%

David S. Kuponiyi, Matthew B. Olajide,
Michael A. Eko, Charity S. Odeyemi,
Najeem O. Adelakun
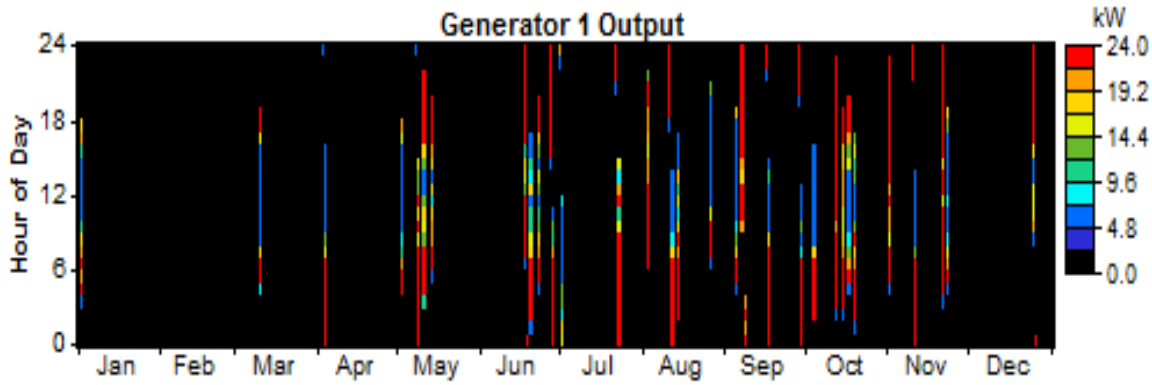
Figure 24 - Generator 1 Output

C. Battery

Table 15: Other Battery Parameters

Quantity	Value
String size	1
Strings in parallel	80
Batteries	80
Bus voltage (V)	6

Table 16: Battery Simulation Result

Quantity	Value	Units
Energy in	42,461	kWh/yr
Energy out	34,066	kWh/yr
Storage depletion	108	kWh/yr
Losses	8,288	kWh/yr
Annual throughput	38,086	kWh/yr
Expected life	12	yr
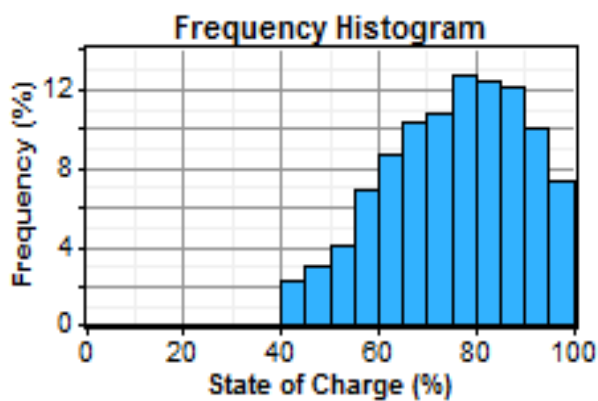
Figure 25 - Battery State of Charge Frequency Histogram
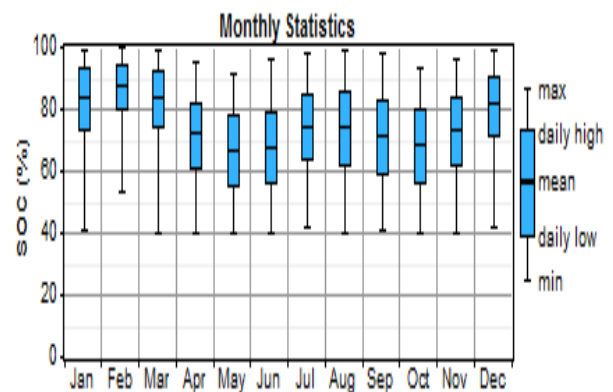
Figure 26 - Battery State of Charge Monthly Statistics
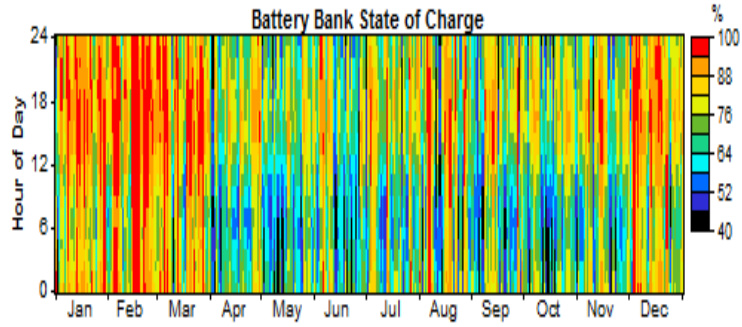
Figure 27 - Battery Bank State of Charge Annual Result

D. Bi-Directional Converter

Table 17: Bi-Directional Converter Output Analysis

Quantity	Inverter	Rectifier	Units
Capacity	20	20	kW
Mean output	5	1.6	kW
Minimum output	0	0	kW
Maximum output	17	19.7	kW
Capacity factor	25.1	7.8	%

Table 18: Bi-Directional Converter Operational Analysis Per Annual

Quantity	Inverter	Rectifier	Units
Hours of operation	5,920	2,054	hrs/yr
Energy in	48,858	16,020	kWh/yr
Energy out	43,972	13,617	kWh/yr
Losses	4,886	2,403	kWh/yr
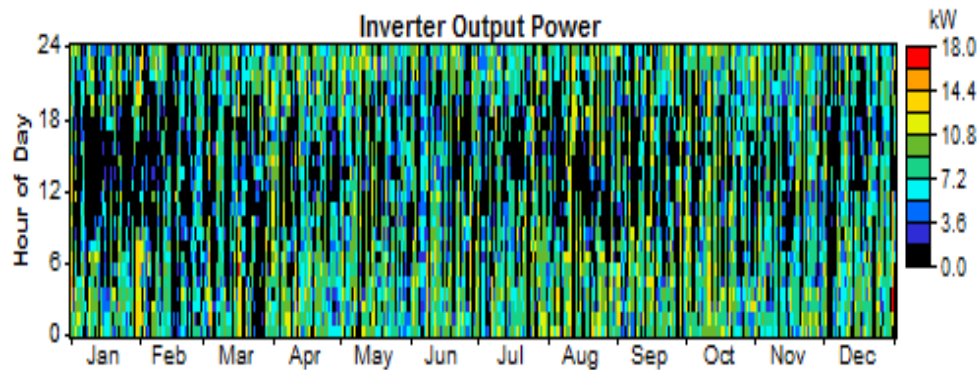
Figure 28 - Bi-Directional – Inverter Output Power
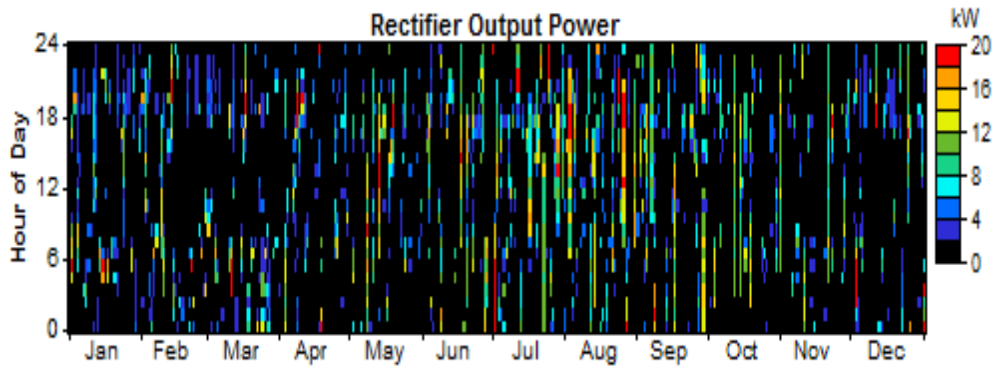
Figure 29 - Bi-Directional Rectifier Output Power

E. Emissions

Table 19: Generator 1 Emission Output

Pollutant	Emissions (kg/yr)
Carbon dioxide	8,141
Carbon monoxide	20.1
Unburned hydocarbons	2.23
Particulate matter	1.51
Sulfur dioxide	16.3
Nitrogen oxides	179
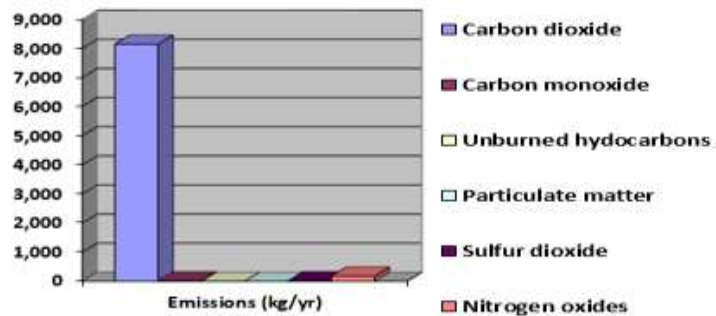
Figure 30 - Generator 1 Emission Output Analysis

Table 20: Optimization Result of Simulation

TOPOLOGY	PV	W.T.	D.G.	BAT.	B.CON	T.C.C.	Total NPC	Operating Cost	COE	Ren. Fraction	Diesel	DGset Hours
	kW	Nr	kW	Nr	kW	₦	₦	₦/yr	₦/kWh		L/yr	hr/yr
OPTION 8	40	2	22	80	20	64,284,000	92,755,080	2,227,170	93.72	0.93	3,077	509
OPTION 7	0	2	22	40	10	33,264,000	102,585,945	5,422,890	103.785	0.55	17,748	2,941
OPTION 6	80	0	22	80	20	66,264,000	105,485,325	3,068,175	106.59	0.86	6,653	1,157
OPTION 5	0	0	22	40	10	18,744,000	134,917,530	9,087,870	136.455	0	32,634	5,268
OPTION 4	0	3	22	0	0	26,004,000	149,226,495	9,639,300	150.81	0.62	26,227	6,902
OPTION 3	30	3	22	0	10	44,979,000	149,559,135	8,181,030	151.14	0.74	21,757	5,843
OPTION 2	60	0	22	0	20	42,174,000	155,230,350	8,844,000	156.915	0.61	24,677	6,387
OPTION 1	0	0	22	0	0	4,224,000	159,794,745	12,169,740	161.535	0	35,168	8,759

4 Conclusion

The optimisation summary table for the eight most cost-effective power systems presented shows the benefits and drawbacks of each model. A comparison of the eight modelled topologies reveals that option one, with solely diesel gensets, has the lowest initial capital cost but the highest running cost, levelized cost of energy, and total net present cost. Option five lacks solar PV and wind turbines but does have storage batteries and inverters, which are common in all rural areas without a national grid. The net present value is 134,917,530:00, a difference of ₦42,162,450:00 from option eight. This analysis also found that option seven, which includes a solar PV system but no wind turbine, is less cost-effective despite having a lower capital cost of nearly half that of option eight. The simulation results proved that if any of the options were properly studied and harnessed, a permanent solution to power failure at our base station would be achieved. Hence, the cost analysis presented shows that the implementation and running costs of any of the options were very low if compared with existing techniques, which will reduce the tariff cost placed on customers. Future research should look at enhanced energy storage technologies, such as next-

David S. Kuponiyi, Matthew B. Olajide,
Michael A. Eko, Charity S. Odeyemi,
Najeem O. Adelakun

generation batteries or supercapacitors, to improve microgrid efficiency. Furthermore, studying the integration of renewable energy sources like solar and wind might lessen dependency on fossil fuels, making Nigerian communication networks more sustainable and environmentally friendly.

References:

[1] Meenual, T. & Usapein, P. Microgrid Policies: 'A Review of Technologies and Key Drivers of Thailand', *Front. Energy Res.*, vol. 9, p. 591537, 2021. https://doi:10.3389/fenrg.2021.591537

[2] Adelakun, N. O. & Olanipekun, B. A. Outage Analysis and System Disturbances on 330 kV and 132 kV Transmission System in Nigeria, European Journal of Engineering Research and Science, Vol. 5, Issue 1. Pp 100-102, 2020. https://doi.org/10.24018/ejers.2020.5.1.1722

[3] Omolola, S.A & Adelakun, N. O. The Relevance of Doubly-Fed Induction Generator (DFIG) in Modelling and Simulation of a Grid Connected Based Wind Turbine System. International Journal of Engineering Technology and Management Science, Vol. 4, Issue 6. Pp 41-47, 2020. http://doi.org/10.46647/ijetms.2020.v04i06.009

[4] Bharath, K. R. Mithun, M. K. & Kanakasabapathy, P. 'A Review on DC Microgrid Control Techniques, Applications and Trends', *Int. J. Renew. Energy Res.*, vol. 9, no. 3, 2019.

[5] Olanipekun, B. A. & Adelakun, N. O. 'Assessment of renewable energy in Nigeria: Challenges and benefits', *Int. J. Eng. Trends Technol.*, vol. 68, no. 1, pp. 64–67, 2020. https://doi:10.14445/22315381/IJETT-V68I1P209

[6] Adelakun, N. O. Omolola, S. A. & Olajide, M. B. 'Off-Grid Renewable Energy Transition in Selected Countries in Africa: Challenges and Opportunities for Sustainable Development', Paper presented at the *2nd Malaysia Sustainability University Network National Conference* 2022, December 6th & 7th, Universiti Putra Malaysia, Malaysia. 2022.

[7] Gao, K. Wang, T. Han, C. Xie, J. Ma, Y. & Peng, R. 'A Review of Optimization of Microgrid Operation', *Energies*, vol. 14, p. 2842, 2021, https://doi.org/10.3390/en14102842

[8] Adelakun N. O. & Olanipekun, B. A. 'A Review of Solar Energy', *J. Multidiscip. Eng. Sci. Technol.*, vol. 6, no. 12, pp. 11344–11347, May 2019, https://doi:10.2139/ssrn.3579939

[9] Oviroh P. O. & Jen, T. 'The Energy Cost Analysis of Hybrid Systems and Diesel Generators in Powering Selected Base Transceiver Station Locations in Nigeria', *Energies*, vol. 11, p. 687, 2018, https://doi:10.3390/en11030687

[10] Kang M. W. & Chung, Y. W. 'An Efficient Energy Saving Scheme for Base Stations in 5G Networks with Separated Data and Control Planes Using Particle Swarm Optimization', *Energies*, vol. 10, no. 9, p. 1417, 2017, https://doi:10.3390/en10091417

[11] Alsharif, M. H. 'Comparative Analysis of Solar-Powered Base Stations for Green Mobile Networks', *Energies*, vol. 10, no. 8, p. 1208, 2017, https://doi:10.3390/en10081208

[12] Tradacete, M. et al., 'Turning Base Transceiver Stations into Scalable and Controllable DC Microgrids Based on a Smart Sensing Strategy', *Sensors*, vol. 21, p. 1202, 2021, https://doi:10.3390/s21041202

[13] Bamisile, O. Qi, H. Hu, W. & Alowolodu, O. 'Smart Micro-Grid: An Immediate Solution to Nigeria's Power Sector Crisis', in *2019 IEEE Innovative Smart Grid Technologies - Asia (ISGT Asia)*, 2019, pp. 3110–3115, https://doi:10.1109/ISGT-Asia.2019.8881774

[14] Suyanto, H. & Irawati, R. 'Study Trends and Challenges of the Development of Microgrids', in 6th IEEE *International Conference on Advanced Logistics and Transport (ICALT)*, 2017, pp. 160–164, https://doi:10.1109/QIR.2017.8168516

[15] Shrivastwa, R. et al., 'Understanding Microgrids and Their Future Trends', 2019, [Online]. Available: https://hal.archives-ouvertes.fr/hal-01973205, (accessed April 15, 2023).

[16] Ghassan, H. Bahjat, E.-D. Mohamad, M. & C, L. A. 'Telecom Infrastructure Sharing Regulatory Enablers and Economic Benefits', 2007.

[17] Nosiri, O. C. Agubor, C. K. Akande, A. O. & Ekwueme, E. U. 'Telecom Infrastructure Sharing, A Panacea for Sustainability, Cost and Network Performance Op-timization in Nigeria Telecom Industry', *Int. J. Sci. Eng. Res.,* vol. 6, no. 8, pp. 621–626, 2015.

[18] Chughtai, O. Badruddin, N. Rehan, M. & Khan, A. 'Congestion Detection and Alleviation in Multihop Wireless Sensor Networks', *Wirel. Commun. Mob. Comput.*, 2017, https://doi:10.1155/2017/9243019

[19] Surajudeen-bakinde, N. T. Adeniji, K. A. Oyeyele, S. O. Zakariyya, Olayanju, O. S. A. & Usman, A. M. 'Assessment of Quality of Service of G.S.M. Networks in Ilorin Metropolis, Nigeria', *ABUAD J. Eng. Res. Dev.,* vol. 3, no. 1, pp. 154–162, 2020.

[20] Nwogbo, K. 'Poor QoS persists 19 years after GSM revolution', Guardian, 2020. https://guardian.ng/technology/poor-qos-persists-19-years-after-gsm-revolution (accessed Mar. 10, 2023).

[21] NCC, '2018 Subscriber/Network Data Report', Niger. Commun. Comm., 2018. (accessed Mar. 12, 2023).

[22] Roy, S. N. 'Energy logic: A road map to reducing energy consumption in telecom munications networks', in IN- TELEC 2008—*2008 IEEE 30th International Telecommunications Energy Conference, San Diego*, CA, USA, 14–18 September, 2008, pp. 1–9.

[23] Busayo, T., Igbekoyi, O., Oluwagbade, O., Adewara, Y., Dagunduro, M., & Boluwaji, Y. Artificial Intelligence and Service Quality of Telecommunication Firms in Nigeria. Journal of Economics, Finance and Accounting Studies, 5(3), 203–214. 2023. https://doi.org/10.32996/jefas.2023.5.3.16

[24] Ayang, A. Videme, B. & Temga, J. 'Power Consumption: Base Stations of Telecommunication in Sahel Zone of Cameroon: Typology Based on the Power Consumption — Model and Energy Savings', *J. Energy*, vol. 2016, 3161060, 2016, https://doi:10.1155/2016/3161060

[25] Anayochukwu A. V. & Ndubueze, N. A. 'Potentials of Optimized Hybrid System in Powering Off-Grid Macro Base Transmitter Station Site', *Int. J. Renew. Energy Res*, vol. 3, no. 4, pp. 861–871, 2013.

[26] Jaiyeola, T. 'Telecom base stations fuel cost rises to N400bn', The Punch, 2023. https://punchng.com/telecom-base-stations-fuel-cost-rises-to-n400bn/ (accessed May 17, 2023).

[27] Ajewole, M. O. Owolawi, & Oyedele, O. M. 'Hybrid renewable energy system for 5G mobile telecommunication applications in', *Niger. J. Pure Appl. Phys*., vol. 8, no. 1, pp. 27–34, 2018, https://doi:10.4314/njpap.v8i1.4

[28] Farret F. A. & Simoes, M. G. 'Micropower System Modeling with Homer', Integr. *Altern. Sources Energy*, IEEE, pp. 379–418, 2006, https://doi:10.1002/0471755621.ch15

Contribution of Individual Authors to the Creation of a Scientific Article (Ghostwriting Policy)

Sources of Funding for Research Presented in a Scientific Article or Scientific Article Itself

Conflict of Interest

Creative Commons Attribution License 4.0 (Attribution 4.0 International, CC BY 4.0)